Comparative Analysis of 12/16 Conventional and Proposed C-core Radial Flux SRM Topologies for In-wheel Electric Vehicle Application

Nikunj Ramanbhai Patel[1*], Varsha Ajit Shah[2], Makarand M. Lokhande[3]
1-Department of Electrical Engineering, Sardar Vallabhbhai National Institute of Technology, Surat, India.
Email: nikunj80_patel@yahoo.com (Corresponding author)
1-Department of Electrical Engineering, Shree Swami Atmanand Saraswati Institute of Technology, Surat, India.
2-Department of Electrical Engineering, Sardar Vallabhbhai National Institute of Technology, Surat, India.
3-Department of Electrical Engineering, Visvesvaraya National Institute of Technology, Nagpur, India.

Received: August 2018 Revised: November 2018 Accepted: January 2019

ABSTRACT:
In in-wheel Electrical Vehicle (EV) applications, Axial Flux Switched Reluctance Motor (AFSRM) is a more suitable solution compared to Radial Flux Switched Reluctance Motor (RFSRM); due to higher outer diameter to axial length ratio with, lower flux length and higher flux density. Switched Reluctance Motor (SRM) attract more attention due to its Permanent Magnet (PM) free structure. In view of this, C-core RFSRM is proposed; which offers combined advantages of radial and axial flux SRM. In this paper, based on a 12/16 pole three-phase structure, C-core RFSRM is compared with conventional RFSRM. Average torque and phase inductance are calculated with mathematical modeling. Computer Added Design (CAD) is verified with 2D and 3D Finite Element (FE) analysis. Based on simulation result, it has been observed that C-core RFSRM offers higher torque compared to conventional RFSRM; with removable wheel/rotor facility, without disturbing the stator. Prototype hardware is designed for feasibility testing of the proposed C-core RFSRM for in-wheel EV applications.

KEYWORDS: Switched Reluctance Motor, Electrical Vehicle, Finite Element Analysis, Flux Line, Radial Field Machine, Axial Field Machine, Advance Motor, Stepper Motor, In-Wheel Application, C-Core.

1. INTRODUCTION

Environmental and economic matters are the major driving force in developing of EV for urban transportation. The selection of traction motor is a key component of EV, with rapid changing in transportation, it increases important of comprehensive understanding of criteria used in motor selection. Currently, Switched Reluctance (SR) machines are predominately used in a diversity of applications in the EV, renewable energy, electrical aircraft, wind turbine and domestic appliances sectors [1], [2]. SRM takes place due to the fact that there are neither field windings nor PM used on the rotor side. As a result, the SRM is low cost and have simple and robust rotor structure compared to other electrical motors. Due to its merits, it is suitable for harsh environment and safety-critical applications. In addition, SRM offers simple structure, ruggedness, high starting torque, fault tolerance ability, high-speed operation, and low manufacturing cost [3-5].

Since 2000, onwards SRM is found suitable for EV. In [6] comparison of different conventional and non-conventional electrical machines for EV applications are presented. First SR motor was used in hybrid electrical vehicle by [7], but significant vibration issues are there. In papers [8], [9], the influence of various stator pole and yoke shapes was investigated and a less vibration structure for 8/6 SRM was proposed. In papers [10], [11] higher torque was achieved by shark pole surface topology and C-core stator design. In [12], duel rotor E-shaped topology is proposed with 20% more torque, but it is bulky structure.

Till now, in EV application 20 to 30 % efficiency is reduced due to mechanical gear system. So as a solution of this, in-wheel motor technique [13] has been come in to the service and motor is developed with new name of "outer rotor hub machine" [14]. In this design stator is situated inside of rotor with stator winding. It has limited space for stator winding with poor heat dissipation. SRM is operating in step so it is also known stepper motor. Due to step operation, there is a torque ripple [15] so for reducing it, axial flux technique [16] comes into the practice.

In axial flux topology, segmented and tooth types poles are mainly developed by [17-19]. Segmented SRM design and FEM Analysis for 3-phase 6/4 pole is proposed in [20]. SRM is a purely magnetic concept so

torque is depending on the setup of number of magnetic line. In [21-24], magnetic analysis of SRM is proposed by mathematical and FE modeling. In [25], prototype model of axial field motor is developed and the issues of low inductance ratio, due to higher leakage flux in SRM by different methods are elicited. In [26-31] various radial and axial flux design techniques has been discussed, for the reduction of torque ripple in SR machines.

Based on this survey, it can be concluded that, by using appropriate control strategy or increasing stator/rotor poles or phase numbers with suitable design technique, torque ripple can be reduced. Issues regarding low power, lower torque density, higher torque ripple and noise are still major challenges in SRM. Several efficacious methods have been investigated to improve the SRM drive system and make it more effective for EV application.

A C-core 12/15 RFSRM was earlier presented in [32] by the author. The same C-core 12/15 RFSRM design is extended in [33] with some required modification by help of mathematical modeling and verified with FEM analysis. A prototype structure of the motor is fabricated, tested and verified with simulation results. This structure has odd number of rotor poles in rotor. In-general odd number of rotor/stator poles are not preferable for conventional radial field motor structure due to magnetic field unbalancing, and it is a limitation of conventional radial field structure.

In this paper, 12/16 pole structure is adopted in place of 12/15 pole for comparing design of conventional RFSRM with design of proposed C-core RFSRM. This paper is arranged as follow:

Electrical dynamics of vehicle, basic machine parameters and magnetic analysis with detailed mathematical modeling for conventional and proposed C-core RFSRM are given in section 2. The geometry comparison of both topologies is also covered in this section. FEM analysis and results of both topologies are compared in section 3. Section 4 contains the conclusion.

2. GEOMETRY AND PARAMETER SELECTION

Flux is perpendicular to the rotating axis in radial flux machine and parallel in axial flux machine. To make the comparison between two radial structures, several parameters are held constant or very near to each other. Complete 3D view of 12/16 pole conventional and C-core RFSRM structures are shown in Fig. 1. To improve the torque density and efficiency with reduction in torque ripple, 12/16 pole SRM configuration is considered. The proposed C-core radial flux machine is designed first to provide the benchmark and then the design of the conventional radial flux machines is attempted.

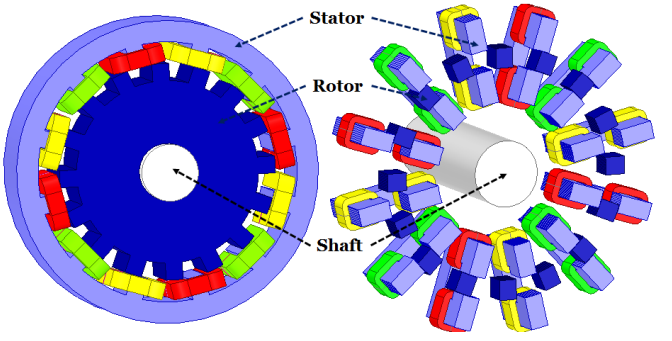

(a) (b)

Fig. 1. 3D view of 12/16 (a) conventional RFSRM (b) proposed C-core RFSRM.

The proposed C-core RFSRM has following merits against conventional RFSRM.

1. All stator cores are magnetically and electrically isolated from each other so it is very easy to wound and maintain.
2. More space available for wound the coils, so it is easy to increase the number of turns.
3. C-core design offers maximum heat dissipation because, the coils are located at outer circumferences. Additional cooling facilities are possible to provide due to the surface mounting.
4. Higher power and torque density: In Proposed C-core RFSRM design, it is easy to increase the radius without increasing the length of magnetic flux line. As a result torque will be increased.
5. Coil length is reduced, due to lower axial length of machine compared to conventional RFSRM. Price will be reduced.
6. Proposed C-core RFSRM structure is fit for in-wheel application for EV. During the maintenance, wheel can be removed by removing four bolts, just like existing vehicle system without disturbing the stator. It is a unique feature of proposed C-core RFSRM over conventional SRM.
7. All time flux is set-up in one direction so reducing the magnetic losses, which occurs due to residual magnetism.

Fig. 2 shows complete geometrical details in Two Dimensional (2D) view. In both of case, stator has 12 pole and rotor has 16 pole. The 12 core of stator carried individual winding which are excited by 3 phases in group on 4 coil. Coils of each phase can be connected in series or parallel. The outer diameter of rotor D_0 is 304 mm. For both types of RFSRM, same area of air-gap is considered as shown in Fig. 3. Rotor teeth/pole length is considered same for similar wind-age losses. The other dimensions like rotor pole arc β_r, stator pole arc β_s, air-gap length l_g, diameter of shaft D_s and axial length of motor are considered same for both cases.

In conventional RFSRM, all rotor poles are part of the single rotor and all stator poles are part of single stator. However, in proposed C-core RFSRM all stator cores and all rotor poles are magnetically and electrically isolated from each other as shown in Fig. 1. CRNO M-45 steel material is considered for all stator and rotor pole. In C-core RFSRM, additionally aluminium disc is required to support the stator cores and rotor poles. The design dimensions are given in Table 1, where some dimensions are assumed based on survey, some are derived by mathematical equation and other are optimized.

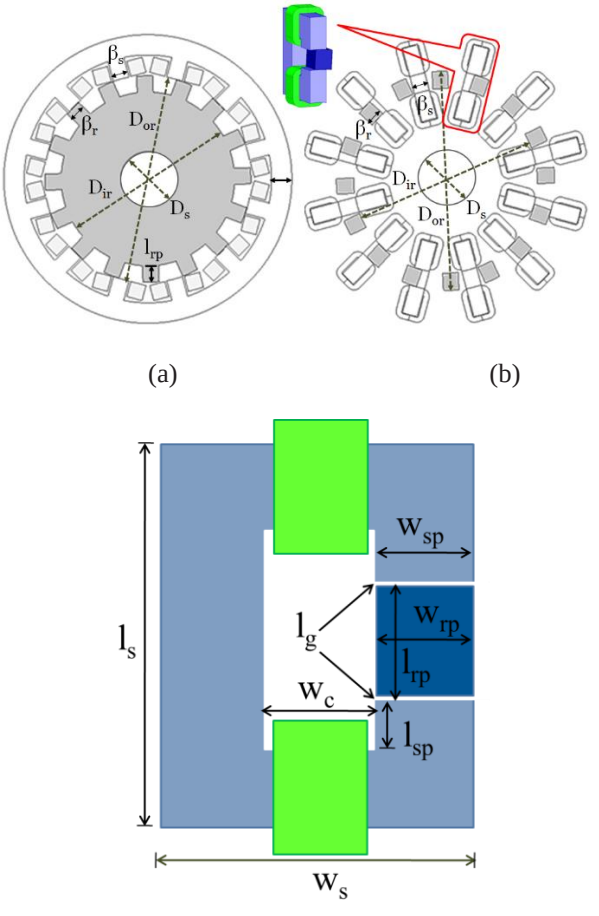

(a) (b)

(c)

Fig. 2. Two dimensional geometric details of (a) conventional RFSRM, (b) proposed C-core RFSRM, and (c) single C-core of proposed C-Core RFSRM.

The design procedure of both topologies is divided into three parts. In the first part, required torque and power are calculated using vehicle dynamic equation. In the second part, the three basic SRM condition and optimized number of stator and rotor poles with arc length are checked by feasible triangle. In the third part, excitation parameters and torque are calculated by using magnetic analysis.

Table 1. Design dimension and rating of conventional and proposed C-core RFSRM.

Parameter	Conventional RFSRM	Proposed C-core RFSRM
Number of stator pole, N_s	12	
Number of rotor pole, N_r	16	
Number of phases, q	3	
Outer diameter of rotor, D_{or}	304 mm	
Inner diameter of rotor, D_{ir}	256 mm	
Total axial length of motor, L	100+A_L mm	
Air-gap length, l_g	0.5 mm	
Diameter of shaft, D_s	80 mm	
Rotor pole pitch, β_{pr}	22.5^0	
Stator pole pitch, β_{ps}	30^0	
Stator pole arc, β_s	9^0	
Rotor pole arc, β_r	9^0	
Stator core length, l_s	-	105 mm
Stator core width, w_s	-	100 mm
Rotor pole length, l_r	24 mm	
Rotor pole width, w_{rp}	30 mm	
Stator pole length, l_{sp}		10 mm
Stator pole width, w_{sp}		30 mm
Coil width, w_c		40 mm
No. of turns per pole	65	
Width of stator yoke, W_{sy}	Depend on length of stator pole arc	Stator core work as a stator yoke (for Individual core)
Rated Speed, N	600 r/min	
Rated current, I	40 A	
Input voltage, V	120 V	

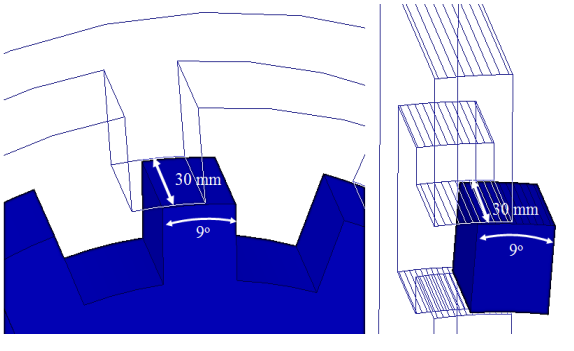

(a) (b)

Fig. 3. Air-gap view of (a) Conventional RFSRM, and (b) C-core RFSRM.

2.1. Modelling of Electrical Vehicle Dynamic

Comparison of two RFSRM is proposed for EV application. Hence the vehicle dynamic parameters need to be considered for the design of RFSRM. The torque demand of vehicle is obtained from the vehicle dynamic equation (1) to design motor. The vehicle torque demanded T_m is a summation of rolling friction, air drag force, effective weight, acceleration and angular acceleration force that is [34]

$$T_m = (\mu mg\cos\psi + \frac{1}{2}v^2\rho AC_d + mg\sin\psi + m\frac{dv}{dt} + \frac{J}{r^2}a)r \quad (1)$$

Where

r : radius of wheel which is 450 mm
μ : coefficient of rolling friction which is 0.0007
ω_m : speed of motor which is 60 km/h ($\omega_m = v/r$)
C_d : drag coefficient which is 0.7
ρ : density of air
A : frontal surface area
v : velocity
ψ : inclination angle
m : mass of vehicle that is 120 kg (for two wheeler)
a: acceleration

As per Indian driving cycle (IDC), acceleration of 0-50 km/h in 20s and speed of 60 km/h are considered. Power requirement of motor is 1.6 kW and torque requirement is 26 N.m. as per vehicle dynamic modelling.

2.2. Rotor and Stator Pole Arc Selection

The number of rotor poles and stator poles are arranged in such a way that, when a phase is energized, rotor must be aligned with the particular phase. At the same time other phase must be in unaligned condition with other rotor pole. So when next phase is energized, the new stable position can be achieved. SRM's condition (2), (3) and (4) are summarized and illustrated by feasible zones as shown in Fig. 4, for 12/16 pole RFSRM. Where these three conditions must be satisfied for selected number of rotor and stator pole to achieve the self-starting with lower torque ripple and good average torque.

$$\varepsilon = 360\times\left(\frac{N_r - N_s}{N_r \times N_s} -\right) \le \beta_s \quad (2)$$

$$\frac{360}{N_r} - \beta_r > \beta_s \quad (3)$$

$$\beta_r \ge \beta_s \quad (4)$$

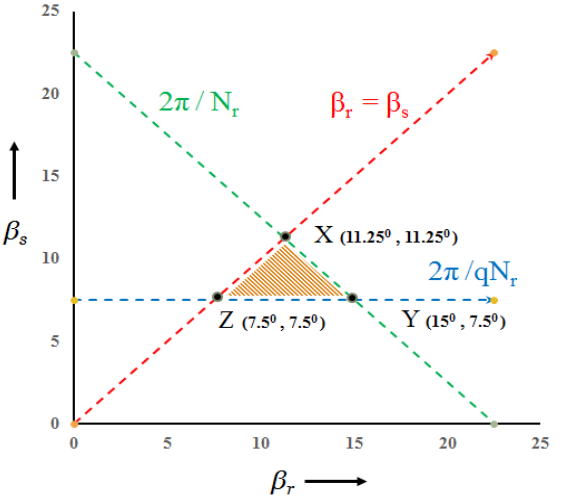

Fig. 4. Feasible zone for stator and rotor pole arc.

Still the feasible zone XYZ is quite big to decide the correct value of stator pole arc β_s and rotor pole arc β_r. According to pulsating field theory of machines, the rotor pole arc is considered 9^0. It is 40 % of rotor pole pitch for maximizing the difference of aligned and unaligned inductance. Now β_s should be less than or equal to 9^0 (4). After the detailed study and based on optometric result, the stator pole arc is considered 9^0. Finally, 7.5^0 step angle is finalized based on feasible triangle to get the highest value of torque with minimum torque ripple. Here dwell angle (β_r - β_s) is considered zero because small dwell angles in min Inductance (L) and max L regions are desirable in $L(\theta)$- θ profile as shown in Fig. 5.

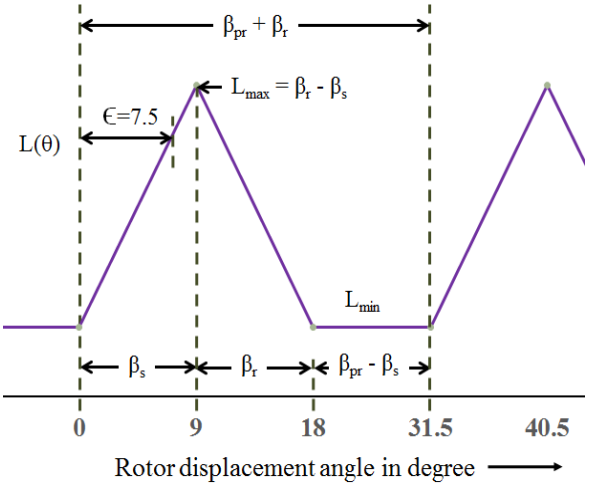

Fig. 5. Idealistic L-θ profile for 12/16 RFSRM.

2.3. Magnetic Analysis of Motor for Aligned and Unaligned Position

For calculating the phase inductance linearised magnetic quivalent model is developed for 12/16 conventional RFSRM and proposed RFSRM as shown in Fig. 6. The reluctance of the yoke, stator pole, air-gap and rotor pole for the flux path are denoted by R_y, R_s, R_g, R_r respectively. Fig. 6 (a) shows the aligned and unaligned Magnetic Equivelent Circuit (MEC) for single phase of conventional 12/16 RFSRM and Fig. 6 (b) shows the aligned and unalined MEC for single pole of praposed 12/16 RFSRM. Four individual pole makes a phase in proposed C-core RFSRM. In both cases, unaligned path is devided into two parallel paths where flux is devided into half from air-gap, as compared to aligned path. For calculation of an inductance at aligned and unalingned, equiflux tubes are defined and calculated the length of line in vaccume and then considered in the account of the iron portions [21]. The air-gap flux can be written as,

$$\phi_g = \frac{MMF}{R_{g(total)}} \tag{5}$$

$$R_g = \frac{l_g}{\mu_0 \times A_g} \tag{6}$$

The airgap area A_g and airgap length l_g are considered same for both 12/16 RFSRM design. So equation of airgap reluctance is approximate same for both cases. Similarly R_y, R_s, and R_r are caculated. The flux density in the air-gap is B_g and can be written as (7) and the magnetic field intensity H_g in the air-gap B_g is given in (8). The magnetic field intensities in stator pole and rotor core are designed as H_s and H_r from B-H charecteristic of M-45 steel material. Here at stator pole maximum flux density is 1.64 T is consider. The number of turns per pole is 50. Group of four poles make an one phase.

$$B_g = \frac{A_s \times B_s}{A_g} \tag{7}$$

$$H_g = \frac{B_g}{\mu_0 \times \mu_r} \tag{8}$$

The phase inductance at aligned position is given by,

$$L_a = \frac{N_{ph} \times \phi_g}{I_p} \tag{9}$$

Where, I_p is peak current. The total unaligned inductance L_u is a sum of all individual flux tube as presented in [33].
The torque equation is given by [1],

$$t = \frac{1}{2} i^2 \frac{dL}{d\theta} \tag{10}$$

By using the calculated value of L_a and Lu, motor average torque is derived as given in Table 2. Here torque is directly proportional of inductance difference between aligned and unaligned position.

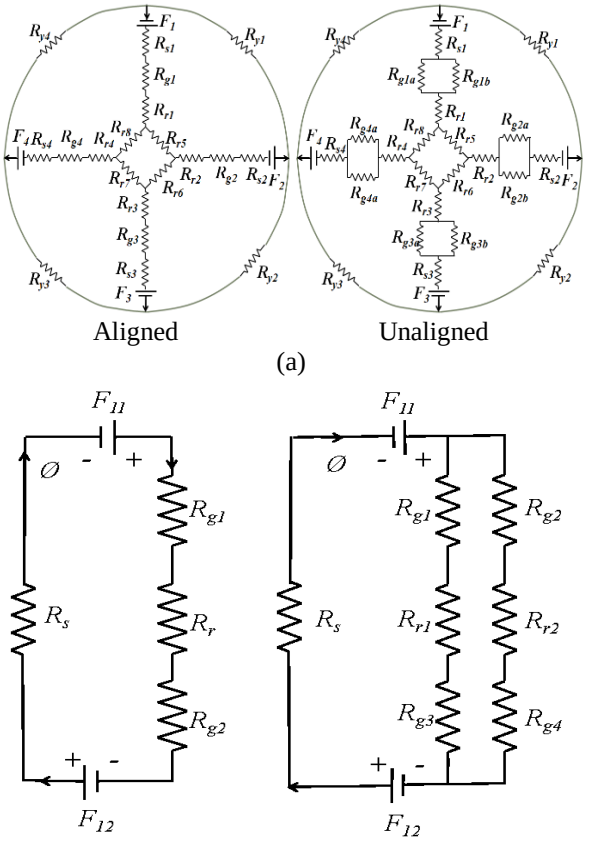

Fig. 6. Magnetic equivalent circuit for 12/16 (a) Conventional RFSRM and (b) Proposed C-core RFSRM.

Table 2. Comparison between two topology using CAD.

	Conventional12/16 RFSRM Design	Proposed C-core 12/16 RFSRM Design
L_a	10.12 mH	6.1 mH
L_u	7.52 mH	1.8 mH
T_{avg}	24 N.m	27.3 N.m

3. FINITE ELEMENT MODEL OF BOTH 12/16 RFSRM

Conventional and proposed C-core 12/16 RFSRM geometries are prepared and analyzed using MAXWELL 2D and 3D FE software. Main dimensions are chosen based on mathematical modeling and analysis as shown in Table 1. Both of the machine's rotor and stator are made by laminated steel stamping. Due to dynamic model and for reducing the simulation time, special care has been taken when assigning mesh. The mesh is assigned in 2D and 3D model as shown in Fig. 7. The status of magnetic flux density at the different parts in stator and rotor pole along with air-gap is shown in Fig. 8. The magnetic flux setup path of conventional RFSRM is longer than proposed C-core RFSRM with same excitation. For proper comparison, 6400 AT MMF/phase is considered in both cases.

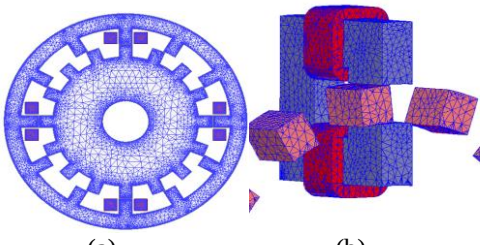

(a) (b)

Fig. 7. Meshing in (a) 2D model of conventional RFSRM and (b) 3D model of proposed C-core RFSRM.

Based on FEM analysis, the average value of air-gap flux density is 1.64 T. In conventional RFSRM, magnetic flux is set-up through two pole and in proposed C-core RFSRM, magnetic flux is setup in individual pole. No additional yoke structure is needed in the proposed C-core RFSRM. Simulated value of aligned inductance and unaligned inductance with average torque of conventional RFSRM and proposed C-core RFSRM are given in Table 3.

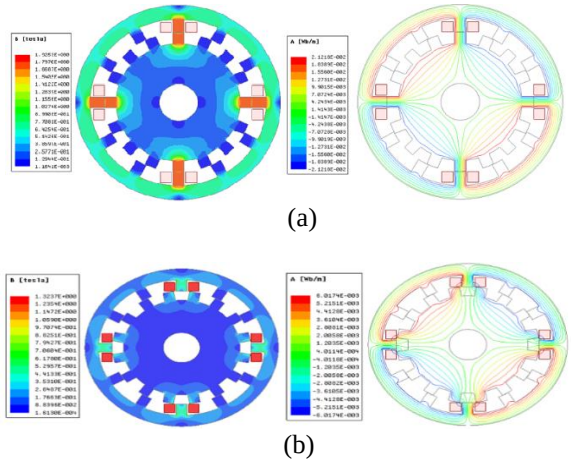

(a)

(b)

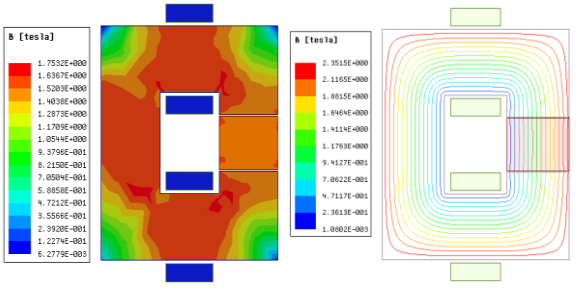

(c)

Fig. 8. Magnetic flux density and field plot of (a) Conventional RFSRM for aligned condition (b) Conventional RFSRM for unaligned condition (c) Proposed C-core RFSRM for single core.

Table 3. Comparison between two topologies by using FEM.

	Conventional 12/16 RFSRM Design	Proposed C-core 12/16 RFSRM Design
La	10.05 mH	6.21 mH
Lu	7.51 mH	1.72 mH
T_{avg}	24.12 N.m	27.4 N.m

The comparison of magnetic characteristics of conventional RFSRM and proposed C-core RFSRM is shown in Fig. 9. In the proposed C-core RFSRM, 20% lesser steel material is required compared to conventional RFSRM. For supporting 12 stator core and 15 rotor pole, additionally non-magnetic material (aluminum) is required in C-core RFSRM. It increases the overall weight of C-core RFSRM compared to conventional RFSRM. In C-core topology, pole windings is divided into two limb, which provide more winding space with good heat dissipation area.

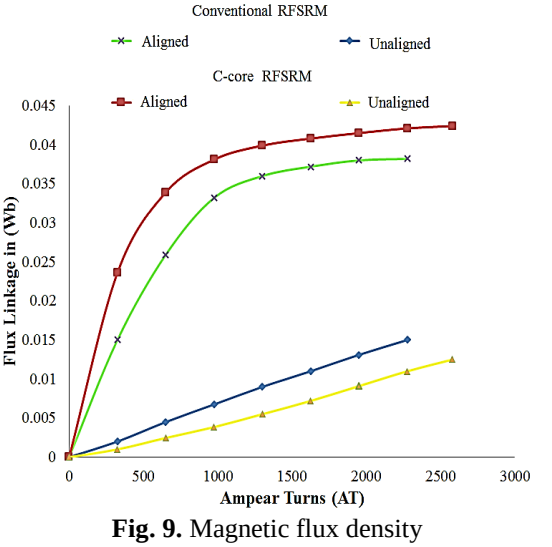

Fig. 9. Magnetic flux density

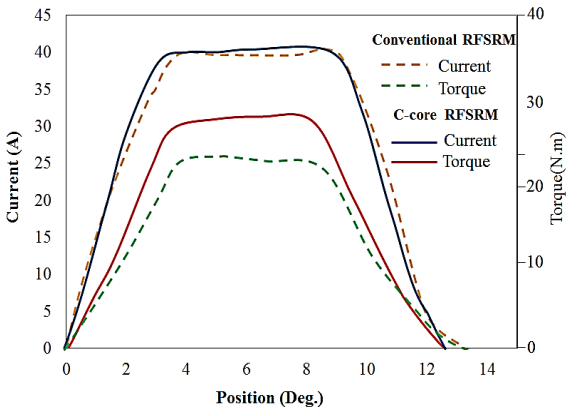

Fig. 10. Comparison of current profile and torque profile for single phase.

It is observed that proposed C-core RFSRM offers good torque due to good aligned to unaligned inductance ratio. It is nearest to 12% higher than conventional RFSRM at rated current as shown in Fig. 10. The step angle of motor is considered 7.5^0 based on rotor and stator pole arc. After every 7.5^0, next phase needs to be energized to achieve the aligned condition to concern phase pole. For exiting the motor, three different phases are exited sequentially by using position sensors.

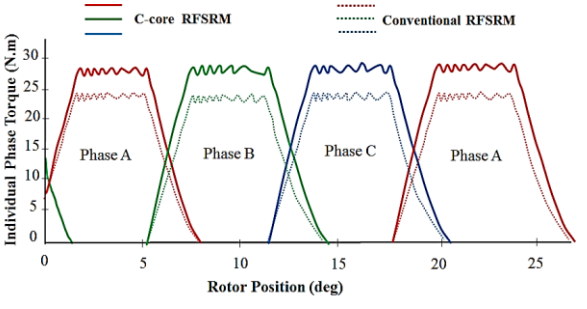

Fig. 11. Comparison of individual phase torque plot between conventional RFSRM and proposed C-core RFSRM.

Fig. 11 shows the comparison between 12/16 Conventional and C-core RFSRM, based on torque characteristics. Where suddenly current fall is noticed at the time of switching the phase.

Fig. 12 shows the variation in torque at different speed of motors. The optimized torque is 27.4 N.m for C-core RFSRM and 24.12 N.m for conventional RFSRM at 600 r/min speed. Fig. 12 shows higher torque with wide speed range at constant power operation around 2-3 times the base speed. In this, before base speed region is representing constant torque zone and after base speed region is representing constant power zone up to the critical speed.

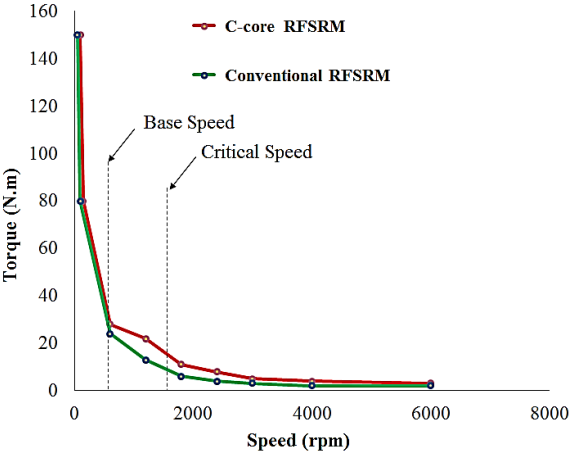

Fig. 12. Comparison of torque on different speed.

After the critical speed torque and power, both are decreased as shown in Fig. 12. The SRM is designed for rated input power capacity of 2.53 kW. For constant torque operation, controller plays the major role. The efficiency map of motor at various speed are given in Fig. 13, it compares two machines based on efficiency. C-core RFSRM is 5% more efficient than conventional RFSRM at rated condition.

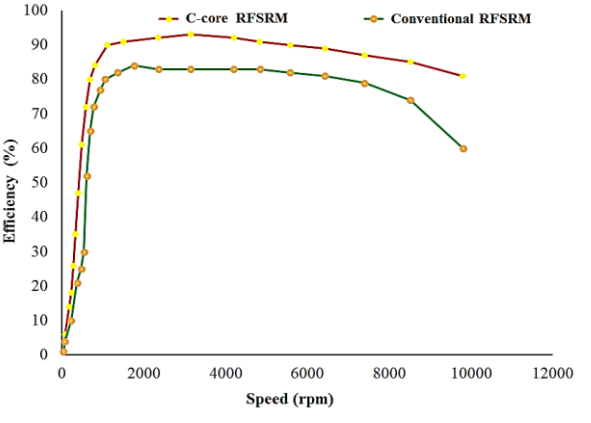

Fig. 13. Comparison of efficiency.

4. IN-WHEEL SUTABILITY FOR ELECTRICAL VEHICLE

In order to improve the efficiency of electrical vehicle, in-wheel motors are mandatory for eliminating the need of a gear box. It also reduces the utilization of space, which increases the compactness. The main features of in-wheel technology is high power density and high efficiency along with rugged construction. Fig. 14 (a) shows the complete view of conventional RFSRM with in-wheel arrangement. In this type of arrangement, wheel is mounted on shaft so torque is reduced. For increasing the torque, gear mechanism is mandatory in such types of inner rotor SRM.

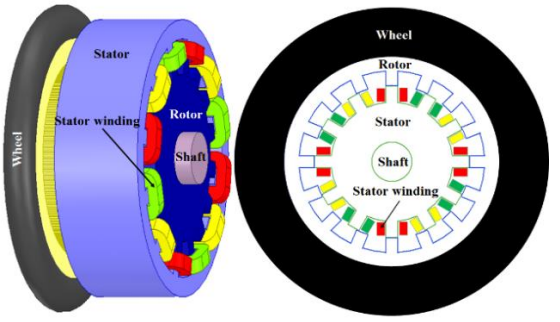

(a) (b)

Fig. 14. (a) Complete view of conventional RFSRM with wheel arrangement. (b) Outer rotor arrangement of conventional 12/16 RFSRM.

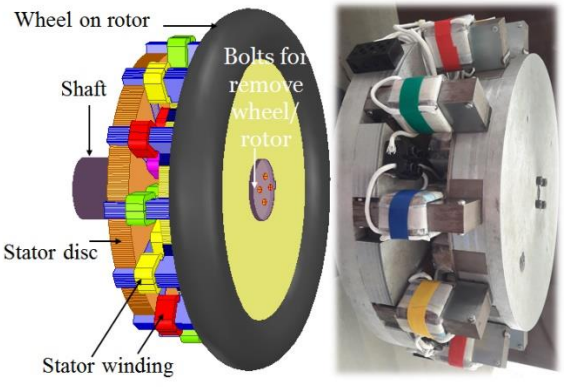

(a) (b)

Fig. 15. Complete (a) view of C-core RFSRM with removable wheel/rotor arrangement. (b) Proto type hardware arrangement of C-core RFSRM.

By transferring rotor at outer periphery, it is possible to implement in-wheel arrangement in conventional RFSRM as shown in Fig. 14 (b). In this type of arrangement, the biggest limitation is small winding space and poor heat dissipation, which is not preferable for higher current density motor. As compared to conventional RFSRM, the proposed C-core RFSRM offers removable wheel structure without disturbing stator. It provides good winding space and heat dissipation area which improve the power handling capability of machine at higher torque and speed. Fig. 15 (a) shows the complete arrangement of 12/16 C-core RFSRM with in-wheel implementation and Fig. 15 (b) shows the complete hardware with removable wheel structure. In this, wheel/rotor can be removed without disturbing the stator or stator winding. The 12/15 C-core RFSRM hardware is developed and tested by author in [33]. By using same mathematical modeling 12/16 C-core RFSRM is designed and compared with conventional RFSRM and prove that proposed design is more feasible for in- wheel electrical vehicle application with special merits.

5. CONCLUSION

A novel C-core RFSRM topology is compared with conventional RFSRM for 12/16 pole structure. It has found that C-core RFSRM offers smaller axial length, shorter and independent magnetic flux path, good heat dissipation and easy maintenance with removable rotor/wheel structure. Proposed C-core design offers 12% higher torque, 5% higher efficiency and 20% lower steel consumption compare to conventional RFSRM. This C-core RFSRM is a potential candidate for electrical vehicle application due to its in-wheel arrangement and higher torque and power density.

REFERENCES

[1] T. J. E. Miller, **"Optimal Design of Switched Reluctance Motors,"** *IEEE Trans. Ind. Electron*., Vol. 49, No.1, pp. 15–27, Feb. 2002.

[2] A. L. M. d. Santos, J. Anthonis, F. Naclerio, J. J. C. Gyselinck, H. V. d. Auweraer, and L. C. S. Goes, **"Multiphysics NVH Modeling: Simulation of A Switched Reluctance Motor for an Electric Vehicle,"** *IEEE Trans. Ind. Electron.*, Vol. 61, No. 1, pp. 469–476, Jan. 2014.

[3] M. Takeno, A. Chiba, N. Hoshi, S. Ogasawara, M. Takemoto, and M. A. Rahman**, "Test Results and Torque Improvement of the 50-kW Switched Reluctance Motor Designed for Hybrid Electric Vehicles,"** *IEEE Trans. Ind. Appl.*, Vol. 48, No. 4, pp. 1327–1334, Jul./Aug. 2012.

[4] H. Chen and J. J. Gu, **"Switched Reluctance Motor Drive with External Rotor for Fan in Air Conditioner,"** *IEEE/ASME Trans. Mechatronics*, Vol. 18, No. 5, pp. 1448–1458, Oct. 2013.

[5] V. Valdivia, R. Todd, F. J. Bryan, A. Barrado, A. Lazaro, and A. J. Forsyth, **"Behavioral Modeling of a Switched Reluctance Generator for Aircraft Power Systems,"** *IEEE Trans. Ind. Electron*., Vol. 61, No. 6, pp. 2690–2699, Jun. 2014.

[6] W. Xu, J. Zhu, Y. Guo, **"Applied Superconductivity and Electromagnetic Devices,"** *Proceedings of 2009 IEEE International Conference on Chengdu China*, Sept., 2009.

[7] Lovatt, H.C. **"Optimization of Switched Reluctance Motors for Hybrid Electric Vehicles,"** *Power Electronics, Machines and Drives, International Conference*, Publ. No. 487, pp. 177 – 182, 2002.

[8] J. Hong **"Stator Pole and Yoke Design for Vibration Reduction of Switched Reluctance Motor,"** *IEEE Trans. on Magn.*, Vol. 38, No. 2, March 2002, pp. 929.

[9] Jian Li, Xueguan Song, **"Comparison of 12/8 and 6/4 Switched Reluctance Motor: Noise and Vibration Aspects,"** *IEEE Trans. on Magn.*, Vol. 44, N0. 11, Nov. 2008, pp. 4131.

[10] J. Corda, A.M. Tataru, P.O. Rasmussen and E. Ritchie, **"Analytical Estimation of Torque Enhancement of the SR Machine with Saw-Shaped (Shark) Pole Surfaces,"** *IEE Proc.-Electr. Power Appl.*, Vol. 151, No. 2, March 2004.

[11] Sh. H. Mao, M. Ch. Tsai, **"Novel Switched Reluctance Motor with C-Core Stators,"** *IEEE Transactions on Magn*, Vol. 41, No. 12, pp. 413, Dec.

2005.

[12] W. Yang, **"Design and Research of a New Dual-Rotor Switched Reluctance Motor for Hybrid Electric Vehicles,"** *Electrical Machines and Systems (ICEMS*), *International Conference*, pp. 829 – 833, 2010.

[13] W. Yaling, "**Outer-rotor Switched Reluctance Motor and Its Control System Used in Electric Vehicles",** *Electrical Machines and Systems (ICEMS), International Conference*, pp. 1 – 4, 2011.

[14] Sakthivel, P., "**Design of a 250 w, Low Speed Switched Reluctance Hub Motor for Two Wheelers,"** *Electrical Energy Systems (ICEES), 1st International Conference*, pp. 176 – 181,2011.

[15] R. Madhavan and B.G. Fernandes, **"A Novel Technique for Minimizing Torque Ripple in Axial Flux Segmented Rotor SRM,"** *IEEE Conference, Energy Conversion Congress and Exposition (ECCE)*, pp. 3383 – 3390, 2011.

[16] B. G. Fernandes, **"A Novel Axial Flux Segmented SRM for Electric Vehicle Application,"** *XIX International IEEE Conference on Electrical Machines – ICEM*, pp 1-6. Sept. 2010.

[17] S. Khaliq, M. Modarres, Thomas A. Lipo**, "Design of Novel Axial-Flux Dual Stator Doubly Fed Reluctance Machine,"** *IEEE Trans. on magn.,* Vol. 51, No. 11, pp. 804-807, Nov. 2015

[18] Fernandes B.G., **"Comparative Analysis of Axial Flux SRM Topologies for Electric Vehicle Application,"** *Power Electronics, Drives and Energy Systems (PEDES), IEEE International Conference*, pp. 1 – 6, Dec.2012.

[19] Madhavan R., **"Axial Flux Segmented SRM with a Higher Number of Rotor Segments for Electric Vehicles,"** *Energy Conversion, IEEE Transactions*, Vol. 28, No. 1, pp. 203 – 213, 2013.

[20] W. Qinghai, H. Xiaofeng, J. Defei, W. Shasha, Z. Tao, **"Parameter Design and FEM Analysis for 3-phase 6/4 Poles Switched Reluctance Motor,"** *Proceedings of the 30th Chinese Control Conference*, July 2011.

[21] P. Vijayraghavan, **"Design of Switched Reluctance Motors and Development of a Universal Controller for Switched Reluctance and Permanent Magnet Brushless DC Motor Drives,"** *PhD Report, Blacksburg, Virginia*, Nov. 2001.

[22] Ragavan, K., Prathamesh, J., **"A Novel Magnetic-Circuit Based Design Approach for Electric Vehicle Motors,"** *Electric Vehicle Conference (IEVC), IEEE International*, pp. 1 – 5, 2012,

[23] W. Ding, Zh. Yin, Ling Liu, **"Magnetic Circuit Model and Finite-Element Analysis of a Modular Switched Reluctance Machine with E-Core Stators and Multi-Layer Common Rotors,"** *Published in IET Electric Power Applications*, March 2014. ISSN 1751-8660.

[24] T. Kellerer, O. Radler, **"Axial Type Switched Reluctance Motor of Soft Magnetic Composite,"** *Innovative Small Drives and Micro-Motor Systems, GMM/ETG Symposium*, pp. 1 – 6, 2013.

[25] A. Labak, Narayan C. Kar, **"Novel Approaches Towards Leakage Flux Reduction in Axial Flux Switched Reluctance Machines,"** *IEEE Trans. on Magn*, Vol. 49, No. 8, Aug. 2013.

[26] Chiba, Y. Takano, M. Takeno, T. Imakawa, N. Hoshi M. Takemoto, and S. Ogasawara, **"Torque Density and Efficiency Improvements of a Switched Reluctance Motor Without Rare-Earth Material for Hybrid Vehicles,"** *IEEE Trans. Ind. Appl*., vol. 47, no. 3, pp. 1240–1246, May/Jun. 2011.

[27] Y. K. Choi, H. S. Yoon, and C. S. Koh, **"Pole-shape Optimization of a Switched-Reluctance Motor for Torque Ripple Reduction,"** *IEEE Trans. Magn.*, Vol. 43, No. 4, pp. 1797–1800, Apr. 2007.

[28] J. Li, X. Song, and Y. Cho, **"Comparison of 12/8 and 6/4 Switched Reluctance Motor: Noise and Vibration Aspects,"** *IEEE Trans. Magn*., Vol. 44, No. 11, pp. 679–686, Nov. 2008.

[29] A. Siadatan, E. Afjei, **"An 8/6 Two Layers Switched Reluctance Motor: Modeling, Simulation and Experimental Analysis,"** *Majlesi Journal of Electrical Engineering*, Vol. 6, No. 1, March 2012.

[30] T. Higuchi, K. Ueda, and T. Abe, "**Torque Ripple Reduction Control of a Novel Segment Type SRM with 2-steps Slide Rotor,"** *in Proc. IEEE Int. Power Electron. Conf*., pp. 2175–2180, Jun. 2010.

[31] B. Bilgin, A. Emadi, and M. Krishnamurthy, **"Comprehensive Evaluation of the Dynamic Performance of a 6/10 SRM for Traction Application in PHEVs,"** *IEEE Trans. Ind. Electron*., Vol. 60, No. 7, pp. 2564–2575, Jul. 2013.

[32] Nikunj R. Patel, Varsha A. Shah, and Makarand M Lokhande **"Design and Performance Analysis of Axial Flux C-Core Switched Reluctance Motor for In-Wheel Electrical Vehicle Application,"** *IEEE ITEC Conference*, pp 1– 6, June-2016.

[33] Nikunj R. Patel, Varsha A. Shah, and Makarand M Lokhande **"A Novel Approach to the Design and Development of 12/15 Radial Field C-core Switched Reluctance Motor for Implementation in Electric Vehicle Application,"** *IEEE Transactions on Vehicular Technology*, May-2018 [Online Available].

[34] Larminie, J. and Lowry, J., **"Electric Vehicle Technology Explained,"** *John Wiley and Sons ltd*, pp. 186–192, 2003.